J Fluoresc (2009) 19:939–946
DOI 10.1007/s10895-009-0493-8

ORIGINAL PAPER

# The Synthesis of Magnetic and Fluorescent Bi-functional Silica Composite Nanoparticles via Reverse Microemulsion Method

**Guannan Wang · Chao Wang · Wenchao Dou · Qiang Ma · Pingfan Yuan · Xingguang Su**

Received: 7 October 2008 / Accepted: 5 June 2009 / Published online: 23 June 2009


**Abstract** In this paper, a simple synthesis method of small-size( about 50 nm in diameter), high magnetic and fluorescent bi-functional silica composite nanoparticles were developed, in which water-soluble $Fe_3O_4$ magnetic nanoparticlels (MNs) and CdTe quantum dots (QDs) were directly incorporated into a silica shell by reverse micro-emulsion method. The high luminescent QDs can be used as luminescent marker, while the high magnetic MNs allow the manipulation of the bi-functional silica composite nanoparticles by external magnetic field. Poly (dimethyl-diallyl ammonium chloride) was used to balance the electrostatic repulsion between CdTe QDs and silica intermediates to enhance the fluorescence intensity of MNs-QDs/$SiO_2$ composite nanoparticles. The optical property, magnetic property, size characterization of the bi-functional composite nanoparticles were studied by UV-Vis and PL emission spectra, VSM, TEM, SEM. The stabilities toward time, pH and ionic strength and the effect of MNs on the fluorescence properties of bi-functional silica composite nanoparticles were also studied in detail. By modifying the surface of MNs-QDs/$SiO_2$ composite nanoparticles with amino and methylphosphonate groups, biologically functionalized and monodisperse MNs-QDs/$SiO_2$composite nanoparticles can be obtained. In this work, bi-functional composite nanoparticles were conjugated with FITC labeled goat anti-rabbit IgG, to generate novel fluorescent-magnetic-biotargeting tri-functional composite nanoparticles, which can be used in a number of biomedical application.

G. Wang · C. Wang · W. Dou · Q. Ma · P. Yuan · X. Su (✉)
Department of Analytical Chemistry, College of Chemistry,
Jilin University,
Changchun 130012, China
e-mail: suxg@mail.jlu.edu.cn

**Keywords** Bi-functional nanoparticles · Iron oxide magnetic nanoparticlels · Semiconduductor quantum dots · Reverses microemulsion method

## Introduction

In the past decade, iron oxide magnetic nanopaticles (MNs) and semiconduductor quantum dots (QDs) have attracted great research interest. MNs have unique surperparamagnetic properties and exhibit magnetization only in the presence of a magnetic field, which make it have potential applications in data storage technology, separation of biomolecules, and nucleic aicd detachment [1, 2]. QDs are nanoscale spherical particles that have two main advantages compared to organic fluorophores: its unique optical properties, such as excellent photostability and narrow symmetric emission profile with a broad excitation range [3], the other one is its emission wavelength can be tuned by changing the size of QDs and simultaneously allowing many-color QDs to work by a single narrow-band excitation source [4]. Because of excellent advantages, QDs are currently of great interest as emitting materials for biolabeling applications [5, 6]. Many of these applications require the nanoparticles to be chemically stable, uniform in size and well dispersed in liquid medium. As the chemical stability of MNs is pretty poor and QDs are still facing some unsolved problems as follows: ultra-sensitivity of their fluorescence to the surface states, cytotoxicity of heavy metal ions used in the process of synthesis which are released upon photo-oxidation, and chemical and colloidal instabilities in harsh chemical environments [7, 8]. So, they are usually coated with a protection layer, such as dextran polymer [9] or $SiO_2$ [10]. Surface modification of QDs and MNs with silica layer has led to improved stability, low

toxicity, and higher biocompatibility, and protects the QDs against corrosion of the biological buffers. In addition, the rich and well-known surface chemistry of silica makes bioconjugation more convenient [11]. $SiO_2$ has been considered as one of the most ideal material for protection of MNs and QDs.

In fact, coating inorganic nanoparticles with silica has been widely investigated. The well-known stöber method has succeeded in obtaining core-shell structured semiconductor nanocrystals/$SiO_2$ particles [12], iron oxide nanocrystals/ $SiO_2$ [10], and the multi-functional microspheres [13]. Apart from the stöber method, the microemulsion approach can also be used to coat II-VI nanocrystals with silica [14]. Most recently, reverse microemulsion method has started to be addressed. In comparison with the stöber method, the reverse microemulsion method can yield more uniform spheres in the size range of 30–50 nm, the reaction condition of the reverse microemulsion method is relatively robust, and the resulting silica spheres have smoother surfaces [15]. The reverse microemulsion method has been used to fabricate the CdTe/$SiO_2$ [16] and $Fe_3O_4$/$SiO_2$ nanoparticles [17].

Because MNs have excellent magnetic properties and QDs have excellent optical properties, so the nanoparticles embedded with QDs and MNs will have wider application in biomedicine and biology including magnetic separation and detection of cancer cells, bacteria and viruses. Up to the present, very few studies have been carried to synthesize bi-functional magnetic and luminescent nanoparticles [13, 18–23]. The simultaneous encapsulation of both QDs/$SiO_2$ microbeads and MNs/$SiO_2$ microbeads in silica shell has been achieved by stöber method [13], reverse microemlusion [18] and inverse suspension method [19]. More recently, magnetic and florescent silica microspheres were prepared by silica-coated MNs as core, followed by layer-by-layer (LBL) assembly of poly electrolytes and QDs onto the core surfaces, which were then coated with a final silica shell [20]. Numpon Insin and co-workers used silica microspheres as ligand system. QDs and MNs were incorporated onto the ligands, which were then coated with a silica shell [21]. Nie and co-workers demonstrated the simultaneous or sequential doping of both oil-soluble $Fe_3O_4$ nanocrystals and QDs in silica microcapsules, the microbeads were then changed from oil-soluble to water-soluble by the addition of surfactants [22]. Reverse microemulsion method was employed by Rong He et al. to prepare the bi-functional nanoparticles embedded with MNs and QDs [23]. To our knowledge, it is the first time that some characteristics of bi-functional nanoparticles and the effect of MNs on PL intensity were studied in detail for this method.

In this paper, we described the preparation of bi-functional composite nanoparticles by directly using water-soluble $Fe_3O_4$ nanoparticles and QDs nanoparticles as cores, followed by encapsulation with a silica shell via reverse microemulsion method. QDs were obtained by hydrothermal method using mercaptosuccinic acid (MSA) as stabilizer [24]. The preparation of $Fe_3O_4$ nanoparticles was based on co-precipitation of ferrous and ferric ion solutions. With the aim of embedding more CdTe QDs in silica composite nanoparticles, we used poly (dimethyldiallyl ammonium chloride) (PDDA) to balance the electrostatic repulsion between CdTe QDs and silica intermediates. The MNs-QDs/$SiO_2$ composite nanoparticles show good stabilities toward pH and ionic strength. Subsequently, the surface of silica composite nanoparticles was modified with 3-aminopropyltrimethoxysilane (APS) and 3-(trihydroxysilyl)-propylmethylphosphonate (THPMP), and the nanoparticles modified with $–NH_2$ were conjugated with goat anti-rabbit IgG, which showed it potential application in both separation and biolabeling.

## Experimental

### Reagents and chemicals

All chemicals used were of analytical reagent grade and used without further purification. *n*-hexane, tritonX-100, acetone, ethanol were purchased from Tianjin NO. 1 Chemical Reagent Factory. Mercaptosuccinic acid (MSA) (99+ %), poly (dimethyldiallyl ammonium chloride) (PDDA, Mw=70000 g/mol) were obtained from J&K Chemical Corric. Chloride ($FeCl_3 \cdot 6H_2O$) and ferrous chloride ($FeCl_2 \cdot 4H_2O$) were purchased from ACROS. Cyclohexane. Tellurium powder (200 mesh, 99.8%), tetramethylammonium hydroxide (TMA, 25%), $CdCl_2$ (99+ %) and $NaBH_4$ (99%), Tetraethoxysilane (TEOS), 3-aminopropyltrimethoxysilane (APS), and 3-(trihydroxysilyl)-propylmethylphosphonate (THPMP) were purchased from Sigma-Aldrich Chemical Co. FITC labeled goat anti-rabbit IgG (FITC-IgG ) obtained from Beijing Ding Guo Biotechnology Co. FITC-IgG and glutaraldehyde were diluted with PBS to the concentrations used only immediately prior to use. The water used in all experiments had a resistivity higher than 18 MΩ/cm.

### Instrument

Fluorescence spectra were obtained at room temperature using a ShimadzuRF-5301 PC spectro fluorophotometer. UV-Vis absorption spectra were obtained using a Varian GBC Cintra10e UV-Visible spectrometer. To disperse the nanoparticles, a bath ultrasonic cleaner (Autoscience AS 3120, Tianjin, China) was used. In both experiments, a 1 cm path-length quartz cuvette was used to measure the

absorption or fluorescence spectrum. X-ray photoelectron spectroscopy was performed on a PHI5000C ESCA X spectrometer with Cu KR excitation (1686.6 eV). The samples for TEM measurements were obtained by placing one drop of the samples on copper grids coated with carbon. JEOL-1230 transmission electron microscope was then employed for Transmission electron microscopy (TEM) images. and. Scanning electron microscopy (SEM) was carried out on a Philips XL30 microscope, and Hysteresis loops of the samples were obtained from JDM-B vibrating sample magnetometer (VSM).

## Preparation of magenertic iron oxide nanoparticlels

Monodisperse iron oxide dispersion were prepared using the method already described [25]. Briefly, based on the co-precipitation of $Fe^{2+}$ and $Fe^{3+}$ by adding 25% $NH_3{\cdot}H_2O$ into the mixture of iron salts with a molar ratio ($Fe^{3+}$ : $Fe^{2+}$) of 2:1 under vigorous mechanical stirring and $N_2$ protection. After 15 min, the precipitates were isolated from the solution by magnetic decantation and washed three times by water. TMA was added to peptize the magnetic nanoparticles, and then the alkaline ferrofluid was diluted with water. The concentration of the MNs was 5.4 mg/mL

## Preparation of CdTe QD nanoparticlels

The preparation of mercaptosuccinic acids capped water-compatible CdTe nanoparticlels by hydrothermal route has been described in detail in our previous paper [24]. Briefly, fresh NaHTe solution was added to a $N_2$-saturated $CdCl_2$ solution in the presence of mercaptosuccinic acids at pH 11.2 in an ice-water bath. The ratio of [$CdCl_2$]:[MSA]:[NaHTe] was fixed at 1:2.4:0.5. Then the CdTe precursor solution was put into a teflon-lined stainless steel autoclave with a volume of 50 mL. The temperature of autoclave was maintained at 160°C for 50 min. Then it was cooled to room temperature by a hydrocooling process. Stable water compatible mercaptosuccinic acids capped CdTe QDs with emission maximum at 585 nm were obtained and was used in the present experiments. Compared with the fluorescence emission of Rhodamine 6G [26], the luminescence quantum yield of the CdTe QDs used in this study is 75.2 %. The concentration of the CdTe QDs ($1.03\times10^{-5}$M) was calculated according to the method reported by Peng et al [27].

## Preparation of MNs-QDs/$SiO_2$ composite nanoparticles

MNs-QDs/$SiO_2$ composite nanoparticles were prepared by reverse microemulsion method at room temperature. In this method, cyclohexane was used as a continuous phase, TritonX-100 and n-hexanol were used as surfactant and co-surfactant respectively. First of all, 15 ml cyclohexane, 3.6 ml Triton X-100 and 3.6 ml n-hexanol were added to a flask, after stirring for 20 min, 200 μl MNs and 800 μl QDs were added and mixed with continuous stirring. After 30 min, 120 μl $NH_4OH$ and 120 μl PDDA solution (0.075% v/v) were added. To initiate the hydrolysis, 80 μl TEOS was added to the microemulsion system after 20 min, the reaction progressed in the dark for 24 h of stirring. The microemulsion was broken by adding 20 mL of acetone to the reaction system and the resultant precipitate was MNs-QDs/$SiO_2$ composite nanoparticles which were washed in sequence with iso-propyl alcohol, ethanol and water. During each washing procedure, the dispersion of nanoparticles was subjected to precipitate by external magnetic field, followed by decantation of the supernatant and redispersion of the precipitate in the next solvent with the aid of supersonication. Ultimately, aqueous dispersion of MNs-QDs/$SiO_2$ was obtained for further use.

The PL intensity of MNs-QDs/$SiO_2$ composite nanoparticles is determined by the quantity of CdTe QDs embedded in the MNs-QDs/$SiO_2$ composite nanoparticles. During the hydrolysis step of TEOS, the intermediate silica species can carry negative charges, the same with CdTe QDs stabilized by MSA. The electrostatic forces of repulsion between the negatively charges are not negligible, which limit the quantity of CdTe QDs embedded in the MNs-QDs/$SiO_2$ composite nanoparticles. Therefore, PDDA was used to keep the electrostatic balance during the embedded process.

## Surface functionalization of MNs-QDs/$SiO_2$ composite nanoparticles

Surface functionalization of MNs-QDs/$SiO_2$ composite nanoparticles is important for further application as fluorescent biomarkers. To obtain well biocompatibility and dispersibility, the surface of silica-shell was modified with –$NH_2$. 30 μl of aminopropyltris (methyloxy) silane (APS) was injected to graft amine groups on the surface of MNs-QDs/$SiO_2$ composite nanoparticles. In neutral solution, the amino group had a positive charge, and silica groups had negative charges. The amine-modified silica nanoparticles could back bond to the surface silanol groups, which resulted in very low total charges on the silica nanoparticle surface and no driving force existed on the nanoparticle surface to keep them separated. The excessive APS will cause aggregation of silica nanoparticles, and will consequently reduce their aqueous dispersibility. Therefore, 80 μl THPMP was added to solve this problem [28]. THPMP contains an inert stabilizing group -methylphosphonate-, which was introduced onto the surface of silica composite nanoparticles. The majority of amino groups electrostatic interact with methylphosphonate groups, which block the aggregation of nanoparticles effectively.

The reaction system was then kept under stirring for one more day. The resultant amine-funcationalized CdTe/$SiO_2$ composite nanoparticles were washed by the same purification procedures as those mentioned above.

### Preparation of fluorescent-magnetic-biotargeting tri-functional nanoparticles

To form the IgG antibody conjugated fluorescent-magnetic-biotargeting tri-functional nanoparticles, the amine-functionalized MNs-QDs/$SiO_2$ nanoparticles were made to react with FITC-IgG by using glutaraldehyde as a coupling reagent [29]. First of all, 100 μl amine-functionalized MNs-QDs/$SiO_2$ composite nanoparticles were added to 100 μl of 1% glutaraldehyde solution. The mixture was vibrated for 30 min at room temperature. After that, the nanoparticles were precipitated by a magnet and washed thrice by PBS (pH=7.4). Then 120 μl FITC-IgG solution was added and incubated with constant shaking for about 2 h. It was then washed three times with PBS to remove excess antibodies. The fluorescent-magnetic-biotargeting tri-functional nanoparticles were obtained.

## Results and discussion

### MNs and QDs nanoparticlels

The MNs which were embedded in the bi-functional nanoparticles should have surperparamagnetic properties. From X-ray diffraction pattern of the MNs prepared in this study (Shown in Fig. 1), it is evident that the peaks at 30.22, 35.54, 43.24, 53.5, 57.36, 62.82, and 74.16 are the characteristic peaks of the $Fe_3O_4$ nanoparticlels, and by using the XRD patterns, the approximate average size of nanoparticles can be estimated by applying the Scherrer formula as follows:

$$D = K\lambda/\beta \cos\theta$$

Where λ is the X-ray wavelength (nm), θ is the Bragg angle, β is the excess line broadening, and K is the constant. Thus the MNs size was estimated to be 10 nm, which is consistent with the result obtained from TEM image of the MNs (shown in Fig. 4c), so the magnetic nanoparticlels have surperparamagnetic properties [30].

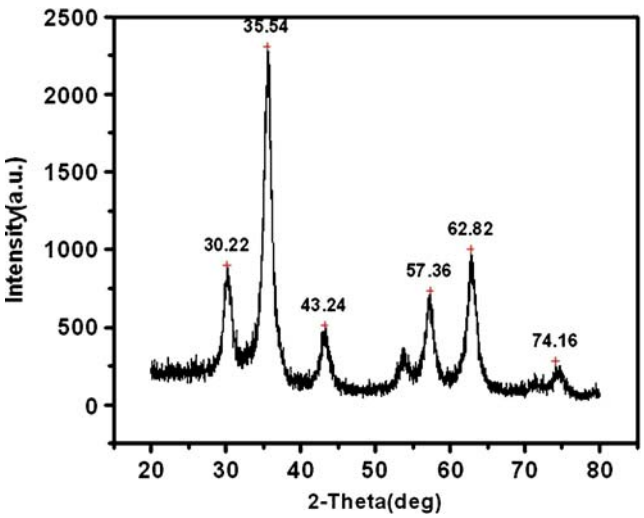


**Fig. 1** Powder XRD patterns of the magnetic $Fe_3O_4$ nanoparticles

The fluorescence emission spectra of the mercaptosuccinic acids-capped water-compatible CdTe nanoparticlels have emission maximum at about 585 nm as can be seen by the results shown in Fig. 2. The relatively narrow PL peak indicates the narrow size distribution of the CdTe QDs and few electronic defect sites.

### Optical property, magnetic property, size characterization of bi-functional nanoparticles

The UV-Vis and PL emission spectra of bi-functional nanoparticles are shown in Fig. 2. Compared with the free QDs in aqueous solution, we can see that after silica coating, the maximum emission peak became blue shift and broader obviously, It had been demonstrated that the blue shift was due to the corrosion of QDs during silica deposition. Since thiol ligands must be completely removed from their surfaces, leaving the QDs unprotected, thus resulting in this blue-shift in the maximum of emission spectra [31].

The magnetic properties of the MNs and bi-functional nanoparticles were studied by using a vibrating sample magnetometer (VSM) with fields up to 10 T. Hysteresis loops of the samples were registered at temperatures of 300 K (Fig. 3). From Fig.3, it can be seen that both of MNs and bi-functional nanoparticles exhibit negligible coercivity (Hc) and remanence, typical of superparamagnetic materials. The bi-functional nanoparticles are superparamagnetic at room temperature, reaching a saturation moment of 13.1 emu per gram of material. This low saturation magnetization value, far less than the saturation magnetization of the MNs used for the preparation of these nanoparticles (55 emu per gram), can be explained by taking into account the diamagnetic contribution of the thick silica shell surrounding the magnetic cores [20].

From SEM image of the MNs-QDs/$SiO_2$ composite nanoparticles (Fig. 4b), it can be seen that the composite nanoparticles had good dispersibility and uniform diameter of about 50 nm, which was further verified by TEM image

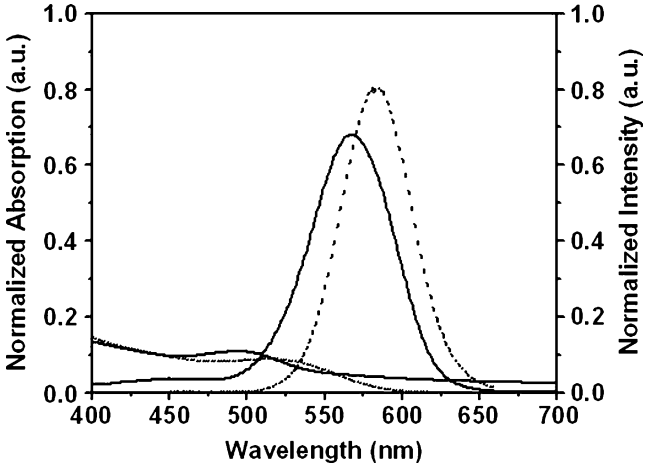


**Fig. 2** Normalized absorption and emission spectra of the solution of CdTe QDs (dashed line) and bi-functional MNs-QDs/$SiO_2$ bi-functional nanoparticles (solid line)

(Fig. 4a). The structure of core-shell of MNs-QDs/$SiO_2$ composite nanoparticles can also been seen from TEM image, which proved the CdTe QDs and MNs were indeed embeded in silica composite nanoparticles. From the photographs of MNs, and bi-functional nanoparticles, driven by an external magnetic field (Fig. 5 a and b), we can see the brown bi-functional nanoparticles were easily manipulated with an external magnetic field. They rapidly responded to the applied magnetic field and get crowded near the point where the magnetic field existed actually. When the magnetic field was removed, the nanoparticles lost their alignments immediately and dispersed again within few seconds by virtue of ultrasonic. All the results

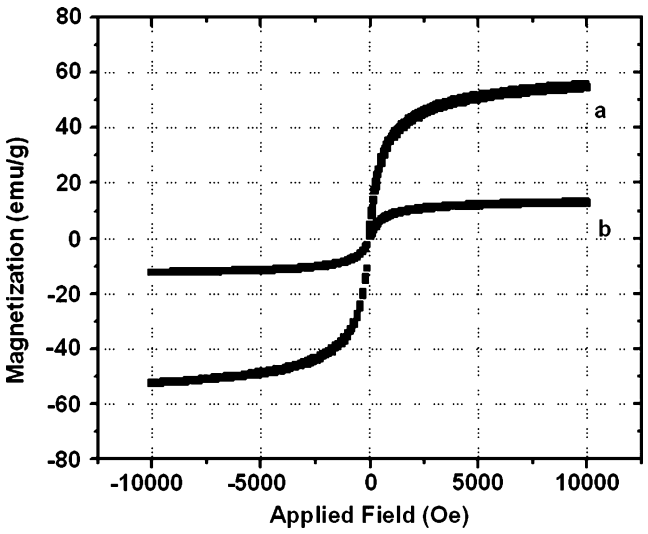


**Fig. 3** Hysteresis loops taken at 300 K for the MNs (**a**) and MNs-QDs/$SiO_2$ bi-functional nanoparticles (**b**)

indicate that the bi-functional nanoparticles can be obtained successfully by reverse microemulsion method.

## Stability of bi-functional nanoparticles

In this paper, we studied the stability of bi-functional nanoparticles in aqueous solution. The results showed that the fluorescence intensity of MNs-QDs/$SiO_2$ composite nanoparticles is remarkably constant over time, keeping their PL intensity even after 20 days without any visible decrease. It indicates that the MNs-QDs/$SiO_2$ composite nanoparticles resisted quenching, the silica shell has a dramatic effect on the stability of the luminescent properties and the surfaces of the nanoparticles are well passivated.

Under physiological condition, ionic strength and pH are the important parameters of the buffer solution. So the influences of pH and ionic strength on the PL properties of MNs-QDs/$SiO_2$ composite nanoparticles and free CdTe QDs were investigated in this study (Figs. 6 and 7). From Fig. 6, it can be seen that pH of buffer largely affects the fluorescence intensity of free QDs and no fluorescence was observed at pH values below than 5, which is due to the precipitation of the QDs [32, 33]. The interaction between a ligand (MSA) and the surface cations can be regarded as a special type of coordinating bond. When hydrogen ions are added into the system, the hydrogen ions will compete for the surface ligands with the nanocrystals. Therefore, the detachment of the ligands from the QD core surface can be considered as a displacement reaction, which will destroy their dispersibility and cause aggregations [33]. As for MNs-QDs/$SiO_2$ composite nanoparticles, it also exhibits high PL intensity when pH is 3.

From Fig. 7, it can be seen that MNs-QDs/$SiO_2$ composite nanoparticles are less susceptible than naked CdTe QDs in different ionic strength solution. The above mentioned results indicate that the PL emission of CdTe QDs can be well protected by the silica network structure when CdTe QDs embedded in silica nanoparticles.

## The effect of MNs on the fluorescence of MNs-QDs/$SiO_2$ composite nanoparticles

To examine the effect of MNs on the fluorescence of MNs-QDs/$SiO_2$ composite nanoparticles, different proportions of MNs were used for preparing MNs-QDs/$SiO_2$ composite nanoparticles, and the fluorescence spectra were recorded correspondingly (Fig. 8). From Fig. 8, it can be seen that with the increasing of the ratios between QDs and MNs from 8:2 (v/v) to 3:7 (v/v), the effect of MNs on the fluorescence of MNs-QDs/$SiO_2$ composite nanoparticles became obviously. The PL intensity gradually decreased and there were a little blue shift in the emission spectra with

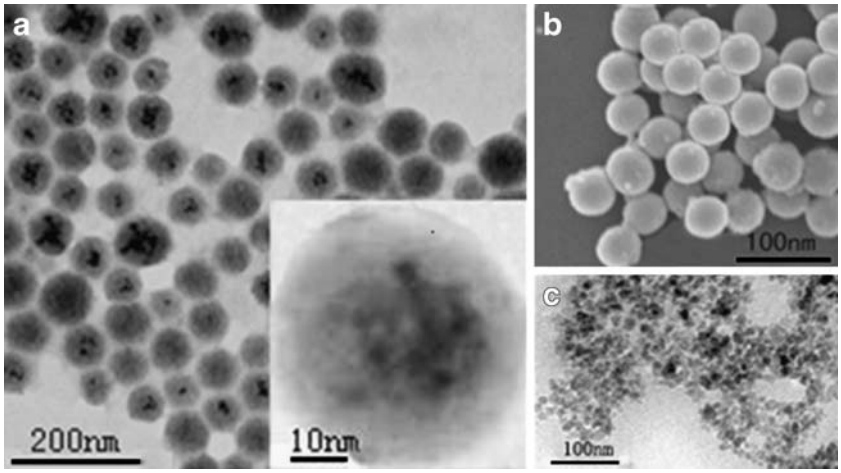


**Fig. 4** TEM images of the MNs-QDs/$SiO_2$ bi-functional nanoparticles (**a**), SEM images of the MNs-QDs/$SiO_2$ bi-functional nanoparticles (**b**), TEM images of the MNs nanoparticles (**c**)

the increase of the proportion of MNs. This phenomenon might be caused by two factors, a broad absorption spectrum of MN in the visible range (400–600 nm), perhaps due to charge-transfer transitions in this mixed valence compound, excitation light in this window will be strongly absorbed by iron oxide, thus attenuating the light intensity reaching the embedded QDs. The other factor responsible for the decreased PL intensity is that with the increasing proportion of MNs, the arrangement of MNs and QDs become more compact, the interaction between MNs and QDs would lead to energy transfer and hence reduce the PL intensity of MNs-QDs/$SiO_2$ composite nanoparticles [34]. This kind of interaction would accelerate the corrosion of QDs during silica deposition, which will induce a blue shift in the emission spectra.

## Bioconjugation and bioactivity

In order to prove the bioactivity of the bi-functional nanoparticles, amine-functionalized MNs-QDs/$SiO_2$ nanoparticles were made to react with FITC-IgG by using glutaraldehyde as a coupling reagent. The fluorescence spectra of the mixture system were shown in Fig. 9. FITC is a green fluorescence dye, which has a maximum emission peak at 520 nm and the maximum emission peak of the bi-functional nanoparticles is at 573 nm. From Fig. 9, it can be seen that the fluorescence spectra of MNs-QDs/$SiO_2$-FITC /IgG system has maximum emission peaks of 520 nm and 573 nm simultaneously, which indicates that the amine-functionalized MNs-QDs/$SiO_2$ composite nanoparticles can be conjugated with IgG to form fluorescent-magnetic-biotargeting tri-functional nanoparticles. It can also be verified by the photographs of fluorescent-magnetic-biotargeting tri-functional nanoparticles driven by an external magnetic field (Fig. 5(c)), From Fig. 5(c), we can see the brown bi-functional nanoparticles were coated with yellow-green FITC-IgG and aggregated at the point where the external magnetic field existed. These also prove the bioactivity of the bi-functional nanoparticles and potential for various applications in separation and bioassay.

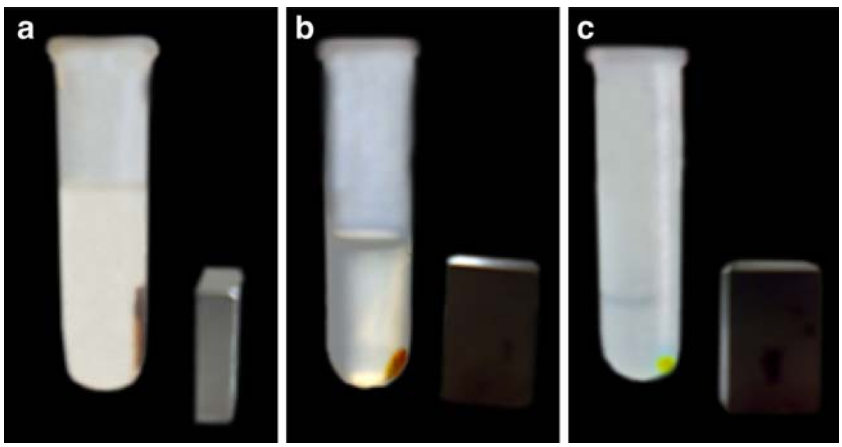


**Fig. 5** Phtographs of MNs (**a**), MNs-QDs/$SiO_2$ bi-functional nanoparticles (**b**), fluorescent-magnetic-biotargeting tri-functional nanoparticles (**c**) driven by an external magnetic field

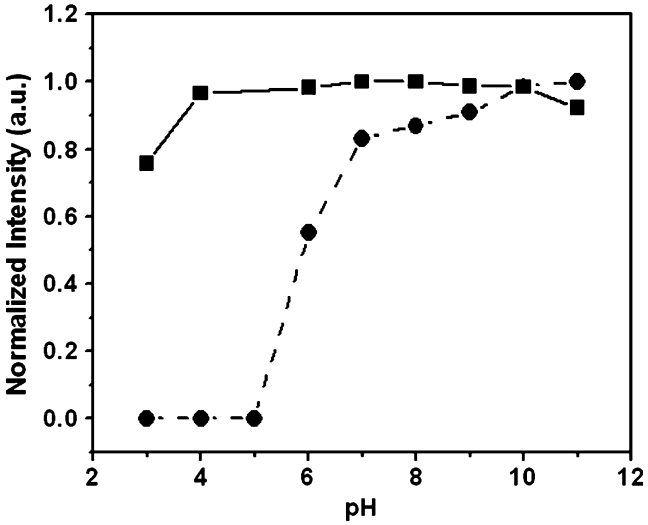


**Fig. 6** Effect of pH on the fluorescent intensity of MNs-QDs/$SiO_2$ bi-functional nanoparticles (solid line) and (dashed line)

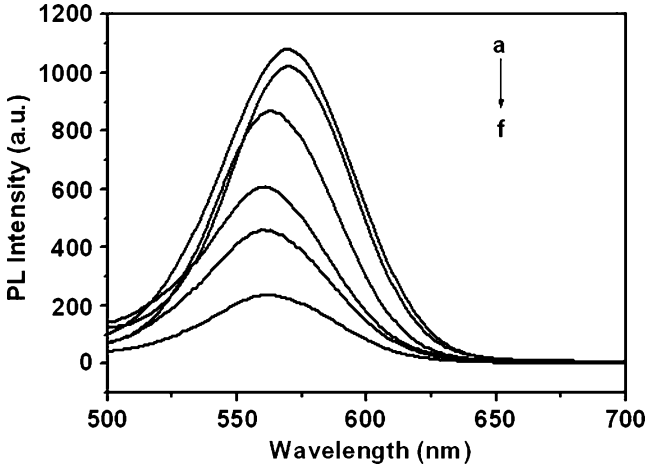


**Fig. 8** Fluorescence emission spectra of MNs-QDs/$SiO_2$ bi-functional nanoparticles with different ratio (V/V) of QDs and MNs:, 8:2 (**a**), 7:3 (**b**), 6:4 (**c**), 5:5 (**d**), 4:6 (**e**), 3:7 (**f**)

## Conclusion

In summary, we synthesized bi-functional nanoparticles by coating aqueous magnetic nanoparticles and CdTe quantum dots with silica shell via reverse microemulsion method. This facile method provides small size (about 50 nm), smooth morphology, high luminescent and magnetic MNs-QDs/$SiO_2$ composite nanoparticles, which have good stability towards time, pH and ionic strength, and can be manipulated easily in the external magnetic field. PDDA was used to keep the electrostatic balance during the process of embedded process. The effect of MNs on the fluorescence of composite nanoparticles was also studied. The surface of the bi-functional nanoparticles was modified with amino group. The modified surface of bi-functional nanoparticles can conjugate with IgG to form fluorescent-magnetic-biotargeting tri-functional nanoparticles, which showed that the modified nanoparticles had good bioactivity. The fluorescent-magnetic-biotargeting tri-functional nanoparticles have potential for detection of bio-molecules such as proteins and targeting agents. The further application of the bi-functional nanoparticles is being developed in our group.

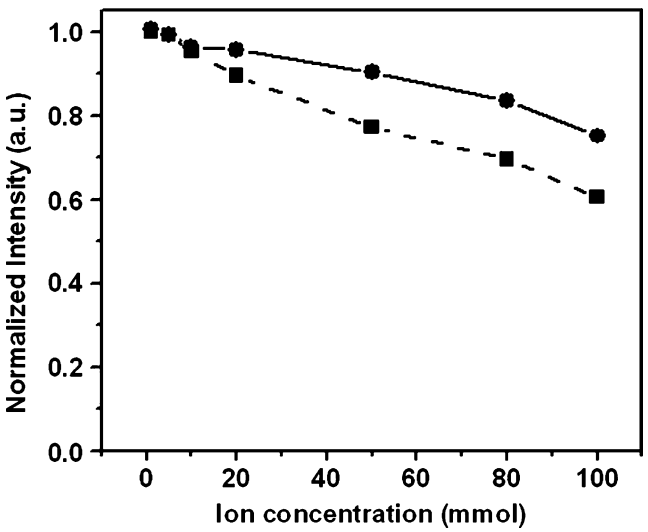


**Fig. 7** Effect of ionic strength on the fluorescent intensity of MNs-QDs/$SiO_2$ bi-functional nanoparticles (solid line) and CdTe QDs (dashed line)

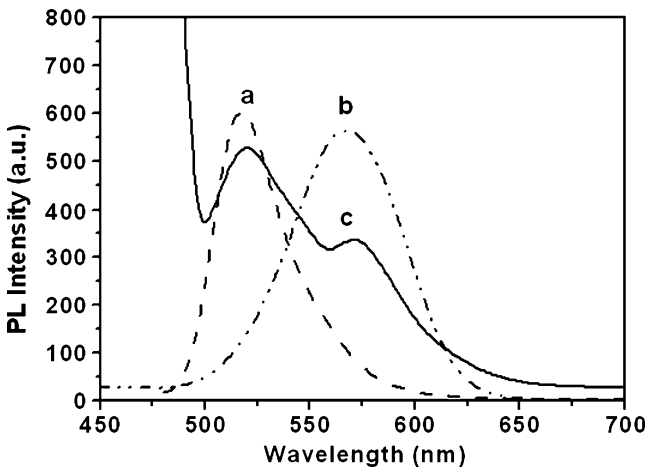


**Fig. 9** The Fluorescence emission spectra of FITC-IgG (**a**), MNs-QDs/$SiO_2$ bi-functional nanoparticles (**b**) and fluorescent-magnetic-biotargeting tri-functional MNs-QDs/$SiO_2$nanoparticles (**c**)

**Acknowledgments** This work was financially supported by the National Natural Science Foundation of China (No. 20475020, No. 20075009, No. 20875036) and the Development Program of the Ministry of Science and Technology of Jilin Province, China (No. 20080544).

## References

1. Al-Hashimi HM, Tolman JR, Majumdar A, Gorin A, Patel DJ (2001) Determining stoichiometry in homomultimeric nucleic acid complexes using magnetic field induced residual dipolar couplings. Chem Soc 123:5806
2. Soh N, Nishiyama H, Asano Y, Imato T, Masadome T, Kurokawa Y (2004) Chemiluminescence sequential injection immunoassay for vitellogenin using magnetic microbeads. Talanta 64:1160
3. Yang YH, Jing LH, Yu XL, Yan DD, Gao MY (2007) Coating aqueous quantum dots with silica via reverse microemulsion method: toward size-controllable and robust fluorescent nanoparticles. Chem Mater 19:4123
4. Mandal SK, Lequeux N, Rotenberg B, Tramier M, Fattaccioli J, Bibette J, Dubertret B (2005) Encapsulation of magnetic and fluorescent nanoparticles in emulsion droplets. Langmuir 21:4175
5. Gerion D, Pinaud F, Williams CS, Parak WJ, Zanchet D, Weiss S, Paul A (2001) Alivisatos synthesis and properties of biocompatible water-soluble silica-coated CdSe/ZnS semiconductor quantum dots. J Phys Chem B 105:8861
6. Mamedova NN, Kotov NA, Rogach AL, Studer J (2001) Albumin-CdTe nanoparticle bioconjugates: preparation, structure, and interunit energy transfer with antenna effect. Nano Lett 1:281
7. Wang C, Ma Q, Dou WC, Kanwal S, Wang GN, Yuan PF, Su XG (2009) Synthesis of aqueous CdTe quantum dots embedded silica nanoparticles and their applications as fluorescence probes Talanta 77:1358
8. Murray CB, Norris DJ, Bawendi MG (1993) Synthesis and characterization of nearly monodisperse CdE (E=sulfur, selenium, tellurium) semiconductor nanocrystallit. J Am Chem Soc 115:8706
9. Li XZ, Wang L, Zhou C, Guan TT, Li J, Zhang YH (2007) Preliminary studies of application of CdTe nanocrystals and dextran-$Fe_3O_4$ magnetic nanoparticles in sandwich immunoassay. Clinica Chimica Acta 378:168
10. Lu Y, Yin YD, Mayers BT, Xia YN (2002) Modifying the surface properties of superparamagnetic iron oxide nanoparticles through a sol-gel approach. Nano Lett 2:183
11. Ulman A (1996) Formation and structure of self-assembled monolayers. Chem Rev 96:1533
12. Correa-Duarte MA, Giersig M, Liz-Marzán LM (1998) Stabilization of CdS semiconductor nanoparticles against photodegradation by a silica coating procedure. Chem Phys Letter 286:497
13. Kim J, Lee JE et al (2006) Magnetic fluorescent delivery vehicle using uniform mesoporous silica spheres embedded with monodisperse magnetic and semiconductor nanocrystals. J Am Chem Soc 128:688
14. Chang SY, Liu L, Asher SA (1994) Preparation and properties of tailored morphology. Monodisperse colloidal silica-cadmium sulfide nanocomposites. J Am Chem Soc 116:6739
15. Darbandi M, Thomann R, Nann T (2005) Single quantum dots in silica spheres by microemulsion synthesis. Chem Mater 17:5720
16. Selvan ST, Tan TT, Ying JY (2005) Robust, non-cytotoxic, silica-coated CdSe quantum dots with efficient photoluminescence. Adv Mater 17:1620
17. Vestal CR, Zhang ZJ (2003) Synthesis and magnetic characterization of Mn and Co spinel ferrite-silica nanoparticles with tunable magnetic core. Nano Lett 3:1739
18. Yi DK, Selvan ST et al (2005) Silica-coated nanocomposites of magnetic nanoparticles and quantum dots. J Am Chem Soc 127:4990–4991
19. Mŭller-Schulte D, Schmitz-Rode T, Paul B (2005) Ultra-fast synthesis of magnetic and luminescent silica beads for versatile bioanalytical application. J Magn Magn Mater 293:135
20. Salgueiriæo-Maceir V, Correa-Duarte MA, Spasova M, Liz-Marzan LM, Farle M (2006) Composite silica spheres with magnetic and luminescent functionalities. Adv Funct Mater 16:509
21. Insin N, Tracy JB, Lee H, Zimmer JP, Westervelt RM, Bawendi MG. (2008) Incorporation of iron oixde nanoparticles and quantum dots into silica microspheres ACS In press.
22. Sathe TR, Agrawal A, Nie SM (2006) Mesoporous silica beads embedded with semiconductor quantum dots and iron oxide nanocrystals: dual-function microcarriers for optical encoding and magnetic separation. Anal Chem 78:5627
23. He R, You XG, Shao J, Gao F, Pan BF, Cui DX (2007) Core/shell fluorescent magnetic silica-coated composite nanoparticles for bioconjugation. Nanotechnology 18:315601
24. Wang C, Ma Q, Su XG (2008) Synthesis of CdTe nanocrystals with mercaptosuccinic acid as stabilizer. J Nanosci Nanotechnol. In press.
25. Lu ZY, Wang G, Zhuang JQ, Yang WS (2006) Effects of the concentration of tetramethylammonium hydroxide peptizer on the synthesis of $Fe_3O_4/SiO_2$ core/shell nanoparticles. Colloids and Surfaces 278:140
26. Gaponik N, Talapin DV et al (2002) Thiol-capping of CdTe nanocrystals: an alternative to organometallic synthetic routes. J Phys Chem B 106:7177
27. Yu WW, Qu LH, Guo WZ, Peng XG (2003) Experimental determination of the extinction coefficient of CdTe, CdSe, and CdS nanocrystals. Chem Mater 15:2854
28. Bagwe RP, Hilliard LR, Tan WH (2006) Surface modification of silica nanoparticles to reduce aggregation and nonspecific binding. Langmuir 22:4357
29. Chen XL, Zou JL, Zhao TT, Li ZB (2007) Preparation and fluoroimmunoassay application of new red-region fluorescent silica nanoparticle. J Fluoresc 17:235
30. Zhang LD, Mu JM (2001) Nanomaterial and Nanostructure. Science, Bei Jing, p 73
31. Guo J, Yang WL, Wang CC, He J, Chen JY (2006) Poly (*N*-isopropylacrylamide)-coated luminescent/Magnetic silica microspheres: preparation, characterization, and biomedical applications. Chem Mater 18:5554
32. Klaus B, Oliver TB, Nikolai G, Alexander E (2006) Comparative examination of the stability of semiconductor quantum dots in various biochemical buffers. J Phys Chem B 110:1959
33. Zhang Y, Mi L, Wang PN, Ma J, Chen JY (2008) pH-dependent aggregation and photoluminescence behavior of thiol-capped CdTe quantum dots in aqueous solutions. Journal of Luminescence 128:1948
34. Liu B, Xie WX, Wang DP, Huang WH, Yu MJ, Yao AH (2008) Preparation and characterization of magnetic luminescent nanocomposite particles. Materials Lett 62:3014